Article **Journal of Chemical and Physical Energy**
June 2022, Vol.9 No.26 1-7

Microstrip and coplanar lines with graphene

Lineas coplanares y de microcinta con grafeno

MORALES-CENTLA, Nathaniel†´, TORREALBA-MELÉNDEZ, Richard*´, TAMARIZ-FLORES, Edna Iliana´´ and LÓPEZ-LÓPEZ, Mario´

´Benemérita Universidad Autónoma de Puebla, Faculty of Electronics Sciences, Mexico.
´´Benemérita Universidad Autónoma de Puebla, Faculty of Computer Science, Mexico.

ID 1st Author: *Nathaniel, Morales-Centla* / **ORC ID:** 0000-0001-8823-786X, **CVU CONACYT ID:** 1075434

ID 1er Co-author: *Richard, Torrealba-Meléndez* / **ORC ID:** 0000-0001-5138-3281, **CVU CONACYT ID:** 172841

ID 2do Co-author: *Edna Iliana, Tamariz-Flores /* **ORC ID:** 0000-0002-0737-5177, **CVU CONACYT ID:** 172840

ID 3er Co-author: Mario López-López / **ORC ID:** 0000-0003-0267-6947, **CVU CONACYT ID:** 67677

DOI: 10.35429/JCPE.2022.26.9.1.7 Received January 10, 2022; Accepted April 30, 2022

Abstract

This paper presents a study concerning the design of transmission lines using graphene. This study aims to obtain the thickness and conductivity values of graphene. These values were obtained by performing simulations of the skin effect and sheet resistance for different conductivities and thicknesses of graphene. Finally, once the values were obtained, simulations of microstrip and coplanar lines were carried out to analyze the effect of the graphene. In addition, a comparison between graphene lines and copper lines was performed.

Graphene, Skin effect, Sheet resistance, Microwaves

Resumen

En este proyecto se presenta un estudio respecto al uso del grafeno en el diseño de líneas de transmisión con la finalidad de obtener los valores de grosor y conductividad del grafeno para que éste presente una baja resistividad de hoja. Estos valores fueron obtenidos realizando simulaciones del efecto piel y la resistencia de hoja para diferentes conductividades y grosores del grafeno. Finalmente, con los valores obtenidos se realizaron simulaciones de líneas de microcinta y coplanares para analizar el efecto que tiene el grafeno en estos dispositivos. Además, se realizó una comparación de los resultados con líneas diseñadas con cobre.

Grafeno, Efecto piel, Resistencia de hoja, Microondas

Citation: MORALES-CENTLA, Nathaniel, TORREALBA-MELÉNDEZ, Richard, TAMARIZ-FLORES, Edna Iliana and LÓPEZ-LÓPEZ, Mario. Microstrip and coplanar lines with graphene. Journal of Chemical and Physical Energy. 2022. 9-26:1-7.

* Correspondence to the Author (Email: richard.torrealba@correo.buap.mx)
† Researcher contributing as first author

Article
Journal of Chemical and Physical Energy
June 2022, Vol.9 No.26 1-7

Introduction

Today, wireless communications play an essential role in daily life. Most wireless communication systems are in the microwave frequency range. Within these systems, passive devices use different conductive materials, seeking to have low electrical resistance and high conductivity, deposited on rigid or flexible substrates, such as glass, polymers, or fiberglass [1].

One of the materials that have allowed development in recent decades is graphene, thanks to its electrical, mechanical, thermal, and optical properties [2, 3]. Although this material, due to its two-dimensional structure, is limited in applications such as structural materials [2], this characteristic, together with those mentioned above, has allowed development in microwave devices [3, 4], among which are transmission lines, resonators and antennas [5, 6, 7, 10].

Microwaves devices

Microwave devices have different uses, ranging from telecommunications and mobile applications [7] to radar systems [8, 9]. Furthermore, the applications of microwave devices have increased due to the rise of I4.0 and the IoT. Therefore, the challenge of the design of microwave devices is to offer responses that satisfy the requirements of the new ways and systems to communicate.

New methods for obtaining and applying graphene have made this material a good option for microwave devices design. One of the most essential processes is graphene-based printing [5, 10, 11, 12]. In this type of ink, it is possible to be purely graphene or a metal/carbon-based hybrid ink [13], but since in some environments the hybrid ink can generate oxidation, and this would impair conductivity, they have opted for the purely carbon-based ink (graphene) [5, 11]. Another technique is laser-induced graphene (LIG) [14], which is versatile for inducing porous graphene from polymeric substrates.

Making devices with graphene offers several advantages, such as the low cost for its mass implementation, its excellent mechanical resistance [10, 11, 15], being able to use the devices in varied environments without loss of conductivity and being able to combine the graphene with other elements to improve properties [11]. Although graphene is not the best conductor on the market, its advantages over the most used manufacturing materials counteract that part.

Skin effect

The skin effect (δ) is a practical problem in all conductors which consists in the fact that the currents that are flowing on the conductor are restricted to a small area, and the higher the working frequency, the smaller the surface that will be used currents [16], this is better appreciated in

Figure 1.

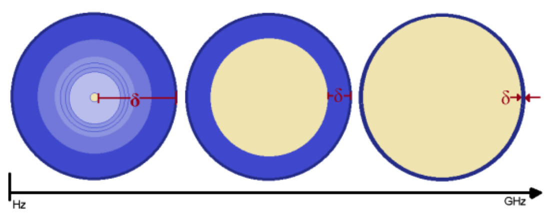

Figure 1 Skin effect on the material

To obtain the value of the skin effect, we use the equation:

$$\delta = \sqrt{\frac{2}{\omega \mu_0 \sigma}} \tag{1}$$

For which it is necessary to know the angular frequency (ω), the conductivity of the material (σ), and permeability in free space (μ_0) [16]. Table 1 shows the value of the skin effect in some materials, varying the frequency.

Skin effect (δ)					
Material	Conductivity(σ), S/m	f=60Hz	f=1KHz	f=1MHz	f=1GHz
Silver	62e6	8.25 mm	2.02 mm	0.064 mm	2.02 μm
Copper	57e6	8.61 mm	2.1 mm	0.067 mm	2.11 μm
Gold	41e6	10.1 mm	2.48 mm	0.79 mm	2.48 μm
Aluminum	38e6	10.5 mm	2.58 mm	0.82 mm	2.58 μm
Steel	10e6	20.5 mm	5.03 mm	0.159 mm	5.03 μm
Graphite	7e4	246 mm	60 mm	1.90 mm	60.1 μm
Silicone	2.3e3	1350 mm	331 mm	10.5 mm	331.9 μm

Table 1 Materials and skin effect

ISSN: 2410-3934

According to Table 1, we can appreciate the effect of the conductivity and the operation frequency over the skin effect. Concerning frequency, skin penetration decreases with frequency increases. Similar behavior occurs when the conductivity increase. For that reason, in this work, we analyzed three graphene conductivity values between 1.02 e4 S/m and 1.1e6 S/m; these are reported in other articles [5, 7, 12, 17, 18, 19]. Figure 2 shows the skin effect for the three graphene conductivity values against the frequency.

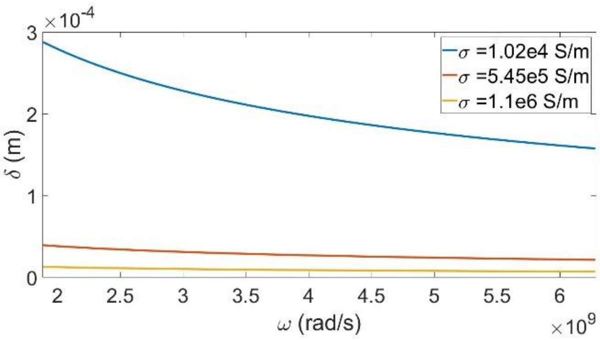

Figure 2 Relation between skin effect and angular frequency

From figure 2, we observed that the skin effect is inversely proportional to the frequency. Besides, we analyzed skin effect versus conductivity behavior for three frequencies in the microwave range, varying the conductivity value, considering the minimum and maximum mentioned above.

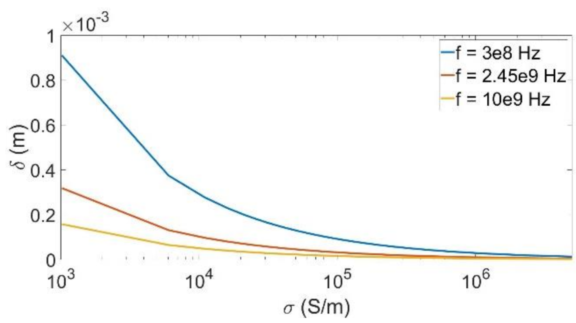

Figure 3 Relation between skin effect and conductivity

Figure 3 shows the behavior of the skin effect concerning conductivity for three frequency values. For the three frequency values, the skin effect decreases with increasing conductivity. The curve for 10GHz presents the lowest values for the skin effect in a range of 0.2 to 0.01 mm.

Correlation between conductivity and sheet resistance

The sheet resistance is a property used particularly in conductors and thin-film semiconductors. This value does not depend on the dimensions of the sheet, which makes a comparison between samples easy [20].

Conductivity is the property of the material for the propagation of heat or electric current. The conductivity is denoted by the letter σ. Also, the inverse of the σ is the electrical resistance represented by ρ [21].

The sheet resistance is denoted by the equation 2 in therm of the ρ.

$$R_{sh} = \frac{\rho}{t} \quad (2)$$

Where:

R_{sh} = Sheet resistance (Ω/sq)

ρ = Resistivity of material (Ω*m)

t = Thickness of material (μm)

Although, in this article, we considered the sheet resistance in terms of conductivity like follow:

$$R_{sh} = \frac{1}{t*\sigma} \quad (3)$$

In the analysis of sheet resistance of the graphene, we use three reported values of thickness of graphene [10, 14] and a conductivity range between 1.02e3 S/m and 5e6 S /m [5, 7, 12, 17, 18, 19]. Figure 4 shows the variation of sheet resistance versus conductivity.

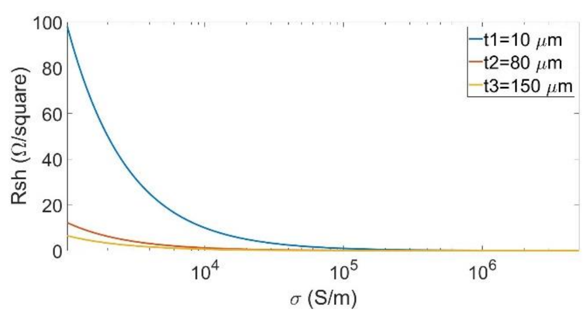

Figure 4 Response of sheet resistance with three thickness

ISSN: 2410-3934

From figure 4, we observe that the sheet resistance decreases with the conductivity increase. Moreover, the skin effect is raised when the thickness of the material is reduced. Therefore, to select a graphene material, we must consider a trade-off between the thickness and conductivity to ensure a low sheet resistance for the graphene.

Microstrip lines

Microstrip lines are composed of a line of conductive material separated from the ground plane by a dielectric, either rigid or flexible [8, 22].

The simulated microstrip line was designed over the glass as substrate with a dielectric permittivity of $\varepsilon_r = 5$ with a thickness of h=1.6mm [14]. The line has an electrical length of 90° for 5GHz and a characteristic impedance of Z0=50Ω**.** The dimensions of the line were calculated employing the following equations.

$$\frac{W}{h} = \frac{8e^{A}}{e^{2A}-2}; \frac{W}{h} \leq 2 \tag{4a}$$

$$\frac{W}{h} = \frac{2}{\pi}\left[B - 1 - \ln(2B-1) + \frac{\varepsilon_r - 1}{\varepsilon_r}\left\{\ln(B-1) + 0.39 - \frac{0.61}{\varepsilon_r}\right\}\right]; \frac{W}{h} > 2 \tag{4b}$$

Where:

$$A = \frac{Z_0}{60}\sqrt{\frac{\varepsilon_r+1}{2}} + \frac{\varepsilon_r-1}{\varepsilon_r+1}\left(0.23 + \frac{0.11}{\varepsilon_r}\right)$$

$$B = \frac{377\pi}{2Z_0\sqrt{\varepsilon_r}}$$

$$\varepsilon_{eff} = \frac{\varepsilon_r+1}{2} + \frac{\varepsilon_r-1}{2}\left(1 + \frac{12h}{W}\right)^{-\frac{1}{2}} \tag{5}$$

The length L of the microstrip lines is calculated by

$$L = \frac{\lambda}{4} = \frac{\left(\frac{c}{f\sqrt{\varepsilon_{eff}}}\right)}{4} \tag{6}$$

The microstrip line was simulated in Sonnet (USA), the thickness of the graphene was set up at t=0.050mm and conductivity of 3700 S/cm. The layout of the microstrip line is presented in Figure 5, and the microstrip dimensions are in table 2.

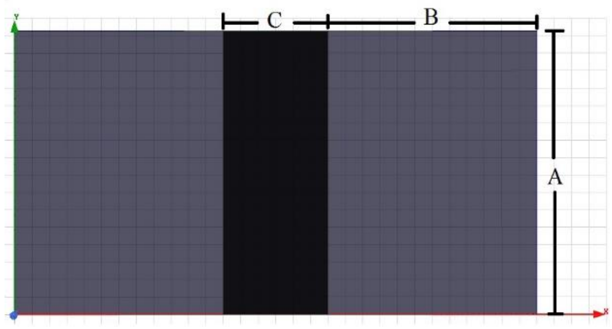

Figure 5 Microstrip line measures

A	B	C
7.78 mm	5.54 mm	2.77mm

Table 2 Measures of Microstrip

To evaluate the behavior of the graphene line, we compared the insertion losses (S21) and return losses (S11) of the graphene against copper lines coefficients. Figures 6 and 7 show these comparisons.

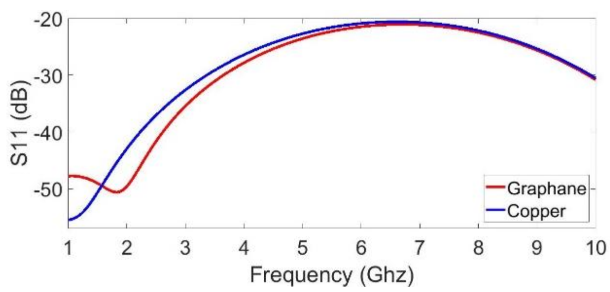

Figure 6 Reflection coefficient response

Figure 6 compares the return losses of microstrip lines with graphene and copper. This comparison was performed in a frequency range of 1 to 10 GHz. The return losses (S11) for the graphene microstrip line present similar behavior and amplitude as the copper microstrip line. In both cases, the S11 is under -20dB.

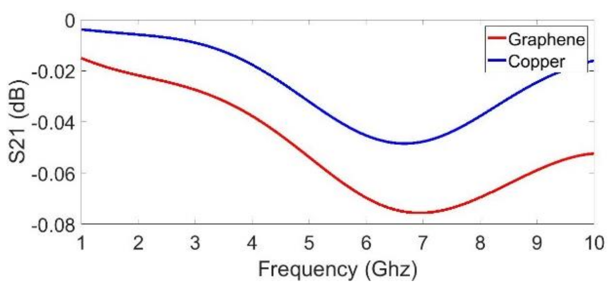

Figure 7 Transmission coefficient response

ISSN: 2410-3934

Figure 6 compares the return losses of microstrip lines with graphene and copper. This comparison was performed in a frequency range of 1 to 10 GHz. The return losses (S11) for the graphene microstrip line present similar behavior and amplitude as the copper microstrip line. In both cases, the S11 is under -20dB.

Figure 7, concerning the insertion losses (S21), the graphene microstrip line presents a higher insertion loss than the copper microstrip line, as shown in Figure 8. This change is due to the difference in conductivity. Insertion loss of the graphene line remains at -0.07 to -0.02dB, while S21 of the copper line is at -0.04 to -0.005dB.

Response of simulation		
Copper		
Freq	S11	S21
1GHz	-55.4902	-0.0038
2.45GHz	-37.5923	-0.0069
5.6 GHz	-21.4119	-0.0409
10 GHz	-30.5344	-0.0160
Graphene		
Freq	S11	S21
1GHz	-47.7863	-0.0150
2.45GHz	-42.4298	-0.0241
5.6 GHz	-22.0879	-0.0640
10 GHz	-30.8236	-0.0524

Table 3 Values obtained from S11 and S21 of copper and graphene

Table 3 summarizes transmission and reflection coefficients in the frequencies 1GHz, 2.45GHz, 5.6GHz, and 10 GHz of the microstrip line with graphene and copper.

Coplanar lines

The coplanar waveguide (CPW) is composed of a conductor and two ground planes located on each side of the conductor with a separation, mounted on a dielectric on the same plane [23].

We take the following values for the simulation of a CPW: as dielectric, we use glass with a dielectric constant of εr= 5 and a thickness of h=1.6mm. The design frequency was 5 GHz. Besides, the line was designed considering an electrical length of 90°, a characteristic impedance Z_0=50Ω, and a value of C=3mm. Figure 8 shows the layout of the CPW line.

To obtain the effective dielectric constant K_{eff}, we use the equation 7 [23]

$$K_{eff} = {}^{\varepsilon_r}/_2 + {}^{1}/_2 \quad (7)$$

The length (A) of CPW was obtained with the equation 6. To avoid resonances higher than the proposal, the value of C+2D must be less than λ/2, and the size of the ground planes (2B) must be at least five times the value of C+2D [24]. Through a parametric analysis based on the principal values, we reduced the weight of the ground plans to 2B=4C. Table 2 presents the calculated dimensions of the CPW line.

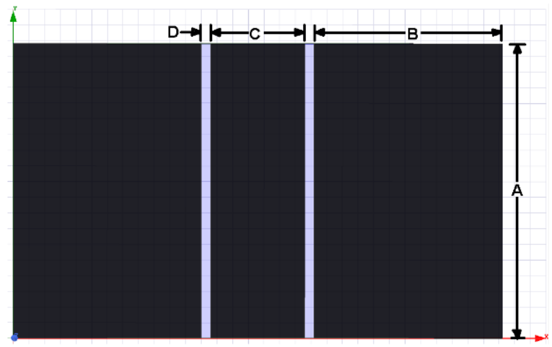

Figure 8 Design of CPW

A	B	C	D
9.4 mm	6 mm	3 mm	0.3 mm

Table 4 Measures of CPW

Two CPW lines were simulated with the last dimension in the HFSS software program. In addition, one line was simulated considering the graphene conductivity of 3700 S/c. The other line was simulated using the copper conductivity of 57e6 S/m. The results of the return losses are shown in

Figure 2, and the insertion losses are shown in

Figure 3.

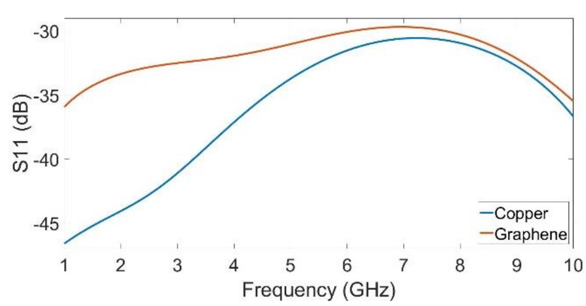

Figure 2 Reflection coefficient response

ISSN: 2410-3934

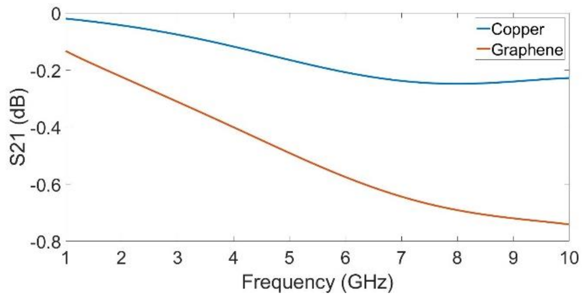

Figure 3 Transmission coefficient response

From Figure 9, the return losses of both lines are under -30dB. The return losses of the CPW line with graphene present a higher level in a range of -35 to -30 dB. However, the return losses of the CPW with cooper are in the range of -45 to -33dB.

However, as in the microstrip line, the CPW line simulated with graphene presents higher insertion losses than the CPW line with cooper. The insertion losses of the CPW graphene line oscillate between -0.7 to -0.15 dB in the simulated frequency range. Table 4 summarizes the insertion and reflection losses for four frequencies.

Response of simulation Copper		
Freq	S11	S21
1GHz	-46.5965	-0.0197
2.45GHz	-42.9147	-0.0569
5.6 GHz	-32.2544	-0.19.17
10 GHz	-36.6859	-0.2279
Graphene		
Freq	S11	S21
1GHz	-35.9347	-0.01332
2.45GHz	-32.8684	-0.02633
5.6 GHz	-30.4198	-0.5428
10 GHz	-35.4867	-0.7412

Table 5 Values obtained from S11 and S21 of copper and graphene

Conclusions

In this article, we can see that graphene is an element that, due to its particular characteristics, can be used for the design of microwave devices as a conductive material and, due to its mechanical properties, it can be deposited on flexible substrates.

Besides, in this paper, we found a trade-off between the conductivity and the thickness of the graphene to obtain low sheet resistance, whit the objective to reduce the insertion losses (S21) of the designed lines.

Funding

This research received no external funding.

References

[1] Bolaños-Torres, M.Á., Torrealba-Meléndez, R., Muñoz-Pacheco, J.M. et al. (2018). Multiband Flexible Antenna for Wearable Personal Communications. *Wireless Pers commun 100*, 1753–1764. https://doi-org.proxydgb.buap.mx/10.1007/s11277-018-5670-0

[2] X. Liu. (2019) Nanomechanics of Graphene and Design of Graphene Composites. *Singapore: Springer Singapore*. https://doi.org/10.1007/978-981-13-8703-6

[3] Y. Zhang, B. Wu, C. Fan, Y. Zhao, S. Sun and X. Liu. (2019). Graphene-based Microwave Planar Devices. *IEEE MTT-S International Wireless Symposium (IWS)*, Guangzhou, China. pp. 1-3, doi: 10.1109/IEEE-IWS.2019.8803939.

[4] M. Yasir, S. Bistarelli, A. Cataldo, M. Bozzi, L. Perregrini and S. Bellucci. (2019). Tunable Phase Shifter Based on Few-Layer Graphene Flakes. *IEEE Microwave and Wireless Components Letters*, vol. 29, no. 1, pp. 47-49, Jan., doi: 10.1109/LMWC.2018.2882309.

[5] K. Pan et al. (2019). Graphene Printed UWB Monopole Antenna for Wireless communication applications. *IEEE International Symposium on Antennas and Propagation and USNC-URSI Radio Science Meeting*, Atlanta, GA, USA, 2019, pp. 1739-1740, doi: 10.1109/APUSNCURSINRSM.2019.8888805.

[6] B. Wu et al. (2020). Dynamically Tunable Filtering Attenuator Based on Graphene Integrated Microstrip Resonators. *IEEE Transactions on Microwave Theory and Techniques*, vol. 68, no. 12, pp. 5270-5278, Dec., doi: 10.1109/TMTT.2020.3017197.

[7] R. Song et al. (2018). Graphene Antenna for Mobile Phone Application. *IEEE International Conference on Computational Electromagnetics (ICCEM)*, pp. 1-2, doi: 10.1109/COMPEM.2018.8496735.

[8] D. M. Pozar. (1998). Microwave Enginnering, *John Wiley & Sons*. ISBN: 978-1-118-29813-8

[9] T. Wayne. (2003). Sistemas de comunicaciones electrónicas, *Pearson educacion*.

[10] J. S. Bunch et al. (2008). Impermeable Atomic Membranes from Graphene Sheets. *Nano Letters*, vol. 8, no. 8, pp. 2458–2462, Aug., doi: 10.1021/nl801457b.

[11] Weijia Wang, Chao Ma, Xingtang Zhang, Jiajia Shen, Nobutaka Hanagata, Jiangtao Huangfu and Mingsheng Xu. (2019). High-performance printable 2.4 GHz graphene-based antenna using water-transferring technology. *Science and Technology of Advanced Materials*. https://www.tandfonline.com/doi/full/10.1080/14686996.2019.1653741

[12] M. Akbari, M. W. A. Khan, M. Hasani, T. Björninen, L. Sydänheimo and L. Ukkonen. (2016). Fabrication and Characterization of Graphene Antenna for Low-Cost and Environmentally Friendly RFID Tags. *IEEE Antennas and Wireless Propagation Letters*, vol. 15, pp. 1569-1572, doi: 10.1109/LAWP.2015.2498944.

[13] N. Curreli et al. (2019). Graphene-based ultra-wide band printed bow-tie antenna for remote tracking. *13th European Conference on Antennas and Propagation (EuCAP)*, Krakow, Poland, pp. 1-4. https://ieeexplore.ieee.org/document/8739804

[14] M. R. R. Abdul-Aziz et al. (2020). Enhancing the Performance of Polygon Monopole Antenna Using Graphene/TMDCs Heterostructures. *IEEE Transactions on Nanotechnology*, vol. 19, pp. 269-273, 2020, doi: 10.1109/TNANO.2974994.

[15] N. Ye et al. (2019). High-Performance Bendable Organic Solar Cells With Silver Nanowire-Graphene Hybrid Electrode. *IEEE Journal of Photovoltaics*, vol. 9, no. 1, pp. 214–219, doi: 10.1109/jphotov.2018.2876998.

[16] J. J. A. B. William H. Hayt. (2001). Engineering electromagnetics, *Boston: McGraw-Hill*.

[17] V. Šlegerytė, D. Belova-Plonienė, A. Katkevičius and D. Plonis. (2019). Microwave Devices With Graphene Layers: A Review. *IEEE Microwave Theory and Techniques in Wireless Communications (MTTW)*, Riga, Latvia, pp. 87-92, doi: 10.1109/MTTW.2019.8897243.

[18] Bartolucci SF, Paras J, Rafiee MA, Rafiee J, Lee S, Kapoor D, Koratkar N. (2011). Graphene–aluminum nanocomposites Mater Sci Eng A 528(27):7933. https://doi.org/10.1016/j.msea.2011.07.043

[19] J. Kumar, B. Basu, F. A. Talukdar and A. Nandi. (2018). Multimode-Inspired Low Cross-Polarization Multiband Antenna Fabricated Using Graphene-Based Conductive Ink. *IEEE Antennas and Wireless Propagation Letters*, vol. 17, no. 10, pp. 1861-1865, doi: 10.1109/LAWP.2018.2868477.

[20] Miccoliet al. (2015). The 100th anniversary of the four-point probe technique: the role of probe geometries in isotropic and anisotropic systems. *J. Phys.: Condens*. Matter 27223201 https://iopscience.iop.org/article/10.1088/0953-8984/27/22/223201

[21] M. R. Haraty, M. Naser-Moghadasi, A. A. Lotfi-Neyestanak and A. Nikfarjam. (2016). Improving the Efficiency of Transparent Antenna Using Gold Nanolayer Deposition. IEEE Antennas and Wireless Propagation Letters, vol. 15, pp. 4-7, doi: 10.1109/LAWP.2015.2424918.

[22] C. A. Balanis. (2005). Antenna Theory Analysis and desing. *John Wiley & Sons*.

[23] R. Simons. (2001). Coplanar Waveguide Circuits, Components, and Systems. *Wiley*. pp. 15-21

[24] Wadell, Brian C. (1991). Transmission line design handbook. Teradyne, pp. 73-79.

ISSN: 2410-3934